Low-cost distributed solar-thermal-electric power generation

A. Der Minassians, K. H. Aschenbach and S. R. Sanders

EECS Department, UC Berkeley, Berkeley, CA 94720, U.S.A.

ABSTRACT

Due to their high relative cost, solar electric energy systems have yet to be exploited on a widespread basis. It is believed in the energy community that a technology similar to photovoltaic (PV), but offered at about \$1/W would lead to widespread deployment at residential and commercial sites. This paper addresses the investigation and feasibility study of a low-cost solar thermal electricity generation technology, suitable for distributed deployment. Specifically, we discuss a system based on nonimaging solar concentrators, integrated with free-piston Stirling engine devices incorporating integrated electric generation. We target concentrator-collector operation at moderate temperatures, in the range of $125°C$ to $150°C$. This temperature is consistent with use of optical concentrators with concentration ratios on the order of 1-2. These low ratio concentrators admit wide angles of radiation acceptance and are thus compatible with no diurnal tracking, and no or only a few seasonal adjustments. Thus, costs and reliability hazards associated with tracking hardware systems are avoided. Further, we note that in the intended application, there is no shortage of incident solar energy, but rather it is the capital cost of the solar-electric system that is most precious. Thus, we outline a strategy for exploiting solar resources in a cost constrained manner. The paper outlines design issues, and a specific design for an appropriately dimensioned free-piston Stirling engine. Only standard low-cost materials and manufacturing methods are required to realize such a machine.

Keywords: Solar Thermal Collectors, Solar Thermal Electricity, Stirling Engine

1. INTRODUCTION

In this paper, we discuss the technical and economic feasibility of a low-cost distributed solar-thermal-electric power generation technology based on the use of a solar thermal collector (STC) in conjunction with a free-piston Stirling engine. The solar thermal collector is to be comprised of low-concentration nonimaging concentrators and absorbers with spectrally selective coatings. The Stirling engine converts moderate temperature heat to electricity by way of integrated electric generation. In spite of its relatively low conversion efficiency, the proposed system can be a cost-effective alternative to solar photovoltaic (PV) modules, as discussed in the sequel.

The system is conceived to operate with collector temperatures in the range of $125°C$ to $150°C$, which is consistent with the use of stationary solar thermal collectors employing low-concentration nonimaging reflectors.[1] Thus, the system avoids the costs and maintenance issues associated with tracking collectors based on high concentration ratio concentrators. However, the use of low temperature heat limits the theoretical maximum thermodynamic efficiency achievable by the heat engine. Although this limits the overall system efficiency, this disadvantage can be compensated for by lower costs in materials and in maintenance.

An operating temperature of $150°C$ permits a maximum thermodynamic (Carnot) efficiency of 29%, assuming the sink temperature is $25°C$. We might reasonably expect the Stirling engine and generator to achieve a thermal-electric efficiency of about 19%, roughly 66% of the Carnot efficiency (see section 3), while the collector operates at a thermal efficiency of about 40%. Thus, the estimated overall efficiency of the system would be about 8%.

We take the view that cost effectiveness of solar electric technologies should be judged by output power per dollar rather than by efficiency or other technical merits. This view reflects the observation that there are

A.D.M.: E-mail: artin@eecs.berkeley.edu; Phone: 1 510 643 5894; Address: 341 Cory Hall, Berkeley, CA 94720, U.S.A.
K.H.A.: E-mail: kaschen@eecs.berkeley.edu; Phone: 1 510 643 5894; Address: 341 Cory Hall, Berkeley, CA 94720, U.S.A.
S.R.S.: E-mail: sanders@eecs.berkeley.edu; Phone: 1 510 642 4425; Address: 565 Cory Hall, Berkeley, CA 94720, U.S.A.

vast untapped siting opportunities in both urban and rural regions of the world. Research into photovoltaics has been focused on improving efficiency because there has been no significant decrease in the inherent cost of silicon wafer area. However, the proposed solar-thermal-electric system is designed for fabrication out of low-cost materials. A collector is built of glass, aluminum, copper, and insulation, while engines and generators are primarily steel, aluminum, copper, and plastics. In high-volume manufacturing, the cost of the proposed system will be determined by the weight of its bulk materials. This study of solar-thermal-electric systems involves searching for a more cost-effective balance between system efficiency and materials cost.

2. POTENTIAL OF STATIONARY SOLAR THERMAL COLLECTORS AND STIRLING ENGINES FOR LOW-COST SOLAR ELECTRICITY

Table 1 compares efficiency and cost for flat panel photovoltaic technology, tracking parabolic trough collector (PTC) technology, and for the discussed low temperature stationary solar thermal conversion technology. Although a case can easily be made to support the cost effectiveness of a tracking-based system, we note such a technology usually needs to be compared with larger scale utility installations. PV modules do not require diurnal tracking and have a peak efficiency of about 15%.[2] Current prices on PV technology suggest they are cost effective on smaller scales at sites where grid electricity is not available.

2.1. System Cost Analysis

The system cost per watt (CPW) of peak electricity output is an important figure of merit for judging cost effectiveness of investment in an electrical generation system. Since investors prefer a short period after which the revenue from energy sold offsets the initial investment, the output power of the system should be maximized for a fixed capital cost. The cost per unit peak output power of the proposed system, CPW_{sys}, is given by

$$CPW_{sys} = CPW_{eng} + \frac{CPA_{STC}}{G_{peak} \cdot \eta_{sys}^{opt}}, \qquad (1)$$

where CPW_{eng} is the engine cost per watt, CPA_{STC} is the collector cost per area (CPA), G_{peak} is the peak solar insolation, and η_{sys}^{opt} is the optimal efficiency of the entire solar-thermal-electric system.

PV modules currently retail for as low as $5 per watt of peak output electrical power.[2] Despite extensive research efforts devoted to increasing their efficiency and lowering their cost, PV modules are unlikely to achieve significant cost reduction due to the cost of silicon. In contrast, solar thermal collectors are primarily comprised of metal formed into simple shapes and coated with appropriate films to reduce optical and thermal losses. One can expect that the cost of collectors and Stirling engine machines will be limited only by material cost in large volume manufacturing. In mature, cost-optimized large-volume industries such as those manufacturing electric motors, automotive parts and other industrial products, the cost of products is proportional to the weight of materials used. Since collectors will dominate the mass of the system, they will dominate the cost of the system in large-scale manufacturing. Assuming that CPW_{eng} is negligible, $G_{peak} = 800$ W/m^2, and $\eta_{sys}^{opt} = 10\%$, the collectors for our system must retail for less than $400/m^2 to match the price of PV technology. A market survey (see Table 4) of stationary collectors for solar heat reveals that several models retail in quantities of 500 m^2 for less than $200/m^2, independent of performance.[3] Furthermore, the materials cost breakdown shown in Table 2 indicates that a representative collector for hot water can easily undercut this cost requirement considering

Table 1. Comparison of solar electric technologies. PTC price is estimate for 500 m^2 of collector only.

System Type	Efficiency [%]	Temperature [°C]	Retail Price [$/W]
Stationary PV[2]	15	N/A	5
Tracking PTC[3]	20	330	1
Stationary STC	8	150	Unknown

Table 2. Materials cost breakdown of Thermo Dynamics G Series STC.[5]

Collector Material	Mass [kg/m^2]	Specific Cost [$/kg]	Cost [$/m^2]
Low-Iron Cover Glazing	7.8	1.87	14.60
Sheet Aluminum	2.75	6.00	16.50
Sheet Copper	1.26	6.35	8.00
Fiberglass Insulation	1.2	0.83	1.00
Total	13	N/A	40.10

economies of scale. Note that specific cost of metals is taken from Ref. 4. Based on the materials cost breakdown in Table 2 and a complete system efficiency of 6.9%, the estimated collector material cost is roughly $0.71/W.

The cost of the Stirling engine can be estimated by calculating the mass of materials used in a prototype design (see section 3). We assume the aluminum parts will be cast in mass production, and that the cost of copper heat exchangers used in the design approaches the cost of the wire used to fabricate them. Table 3 shows the cost of materials used in the prototype Stirling engine design. Given the engine design output power of 200 W, the estimated engine cost is $0.31/W considering economies of scale. Note that cost of metals is taken from Ref. 4. Simple design changes can reduce the amount of structural aluminum used and a new aluminum heat exchanger design can reduce the amount of copper used. We predict that the metals content of the engine can be reduced to almost half, which will further reduce the contribution of the engine to the overall system cost. Further, power density can be increased, as discussed in section 3, resulting in additional cost reduction. Thus, an argument can be made for a complete system cost (collector and engine) in the range of $1/W.

2.2. System Efficiency

The efficiency of a solar thermal collector, η_{STC}, as measured experimentally and approximated with a linear temperature dependence near the desired temperature of operation, is given by

$$\eta_{STC} = \eta_0 - \frac{U}{G}(T_m - T_{amb}), \tag{2}$$

where η_0 is the maximum collector efficiency, U is the thermal loss coefficient, G is the power density of incident sunlight, T_m is the mean temperature of the collector in the Kelvin scale (K), and T_{amb} is the ambient temperature in K. Assuming there is no drop in temperature from the collector to engine, the efficiency of the heat engine, η_{eng}, is given by

$$\eta_{eng} = \epsilon_{Carnot}(1 - \frac{T_{amb}}{T_m}), \tag{3}$$

where ϵ_{Carnot} is the fraction of the theoretical Carnot efficiency that the engine achieves. The system conversion efficiency, η_{sys}, is then given by

$$\eta_{sys} = \eta_{STC} \cdot \eta_{eng}. \tag{4}$$

Table 3. Materials cost breakdown of prototype three-phase Stirling engine.

Engine Material	Mass [kg]	Specific Cost [$/kg]	Cost [$]
Cast Aluminum	4.8	5.50	26.40
Copper Wire	3.5	10.00	35.00
Total	6.9	N/A	61.40

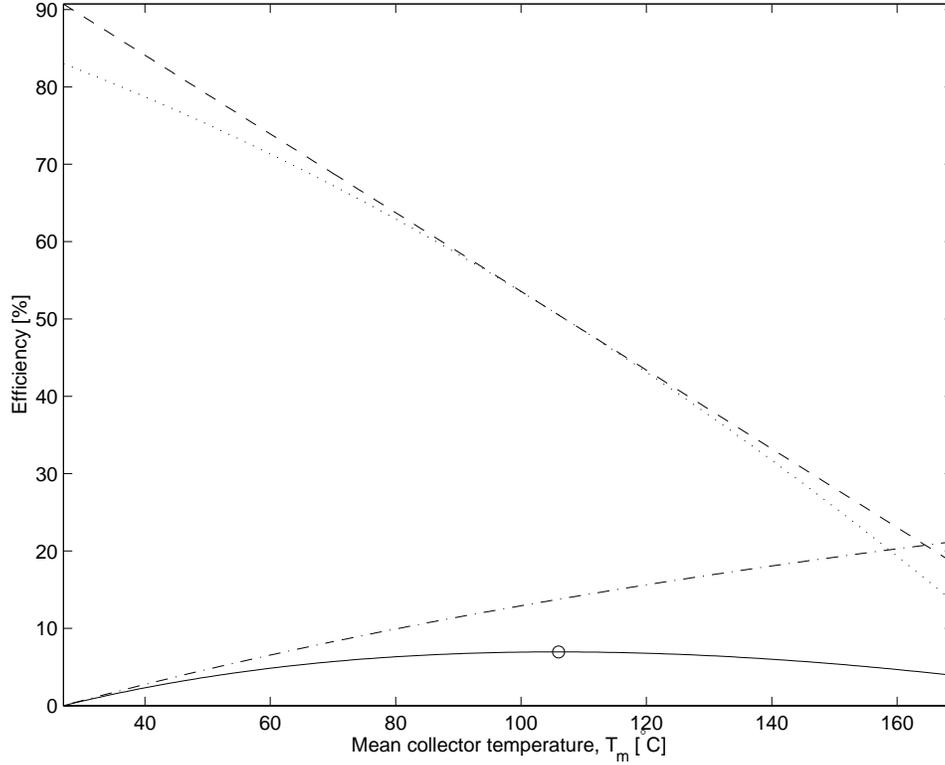**Figure 1.** Efficiency as a function of temperature for a representative system. The parameters used are $\eta_0 = 91\%$, $U = 4.080$ W/m^{2}K, $T_{amb} = 27°$C, and $\epsilon_{Carnot} = 66\%$. The measured collector efficiency is in dotted line, the linearized collector efficiency is in dashed line, the engine efficiency is in dash-dotted line, and the system efficiency is in solid line. The circle indicates the point of optimal system efficiency.

The efficiencies of the collector, engine, and system are plotted as a function of temperature in Fig. 1. At optimal system efficiency, the mean absorber temperature, T_m^{opt}, is given by

$$T_m^{opt} = T_{amb}\sqrt{1 + \frac{\eta_0 \cdot G}{U \cdot T_{amb}}} \quad . \tag{5}$$

The corresponding optimal system efficiency, η_{sys}^{opt}, is given by

$$\eta_{sys}^{opt} = \epsilon_{Carnot}\left(\eta_0 - \frac{U}{G}\left(T_m^{opt} - T_{amb}\right)\right)\left(1 - \frac{T_{amb}}{T_m^{opt}}\right) . \tag{6}$$

To minimize cost per watt of output electricity, it is desirable to operate a system of given cost at the temperature corresponding to peak system efficiency. This temperature is a function of collector properties as well as ambient temperature and intensity of sunlight. The heat engine can be designed to regulate its loading to maintain optimum collector temperature and system efficiency. It is shown in Fig. 1 that the system efficiency is rather flat over a range of temperatures near the extremum. As ϵ_{Carnot} of a practical heat engine is expected to be closer to unity with higher temperatures, the temperature of optimum system efficiency will be somewhat higher than shown.

2.3. Market Available Collectors

Solar thermal collectors generally consist of a transparent cover and selective absorber surface, under which there is tubing to guide heat transfer liquid and insulation to reduce thermal losses. The solar hot water industry has

Table 4. Comparison of market available STCs. The last four columns, from left to right, are computed using Eqs. (5), (2), (6), and (1), respectively. Assumptions: $\epsilon_{Carnot} = 66\%$, $T_{amb} = 27°C$, CPW_{sys} computed assuming engine cost is zero. All costs are approximated by discounted retail price of 500 m^2 collector area.

Collector Model	η_0 [%]	U [W/m^{2}K]	CPA_{STC} [$/m^2]	T_m^{opt} [°C]	η_{STC}^{opt} [%]	η_{sys}^{opt} [%]	CPW_{sys} [$/W]
Flat Plate Collectors							
Thermo Dynamics G Series	74	5.247	194	79	40	3.9	6.27
Arcon HT	79	3.796	142	101	44	5.8	3.07
HFE Solar Eurostart Sc	86	5.180	174	87	47	5.2	4.20
Sonnenkraft GK6	88	5.487	145	85	48	5.1	3.52
Solarnetix FC-25	85	4.840	150	91	47	5.4	3.48
CPC-based Collectors							
AOSOL CPC 1.5X	75	4.280	158	90	41	4.7	4.16
SOLEL CPC 2000 1.2X	91	4.080	193	106	51	6.9	3.49

improved upon flat plate collectors by reducing optical and thermal losses by using high transmission covers and selective absorber materials. More recent designs have employed nonimaging compound parabolic concentrator (CPC) reflectors to improve collector performance. For a small sacrifice in maximum collector efficiency due to imperfect reflector surfaces, CPCs effect a reduction in thermal losses in proportion to the concentration ratio. At the higher temperatures produced by concentration, the thermal ineffectiveness of the engine's heat exchangers have less negative effect on the engine efficiency. Furthermore, since the reflector can be much thinner and lighter than the absorber plate it obviates, the collector cost per unit area can be substantially reduced. We envision a system using collectors based on low-cost truncated 2D CPCs with concentration ratio of about 1.5. The large acceptance angle associated with such a CPC will allow for sufficient hours of operation over all seasons without any tilt adjustments. A representative CPC-based collector would be the SOLEL CPC 2000 trough array, for which the concentration ratio is 1.2, η_0=91% and U= 4.080 W/m^{2}K.[6] An ideal heat engine powered by this collector would run at $T_m^{opt} = 106°C$ and $\eta_{sys}^{opt} = 10.5\%$, whereas a more practical engine would result in perhaps η_{sys}^{opt}=6.9%. Table 4 compares the technical and economic performance of several commercially produced flat plate and CPC-based solar thermal collectors.[3] Although many of these collectors are already shown to be cost-effective at retail prices, the production cost of such collectors is expected to be much lower.

3. STIRLING ENGINE

The Stirling Engine has been in existence for many years, spread over two centuries. The research and development on Stirling cycle machines has been documented in open literature such as Refs. 7, 8, 9 and 10. The Stirling engine converts heat to mechanical power in a manner similar to other mechanical engines, that is, by compressing a working gas when it is cold, heating the compressed working gas, and then expanding it with a power piston to produce work. The Stirling engine works on a closed cycle with a gaseous working fluid that may have a nominal working pressure many times that of atmospheric pressure.[7]

In this paper we focus on free-piston Stirling engines rather than machines incorporating conventional crank mechanisms. Removal of the mechanical crank mechanism reduces frictional losses, complexity, and associated maintenance requirements. Our interest is more narrowly focused on free-piston machines that directly drive electrical generation devices. With this arrangement, we note the following advantageous features. There is no need for any mechanical coupling from the motional elements to the outside of the pressurized container. Thus, there is no emphasis on difficult sealing requirements that have plagued conventional crank mechanism Stirling designs. And, consequently, we anticipate essentially zero leakage of working fluid, allowing long-term maintenance free operation with the fluid pressurized to the level required by the application. A further advantageous
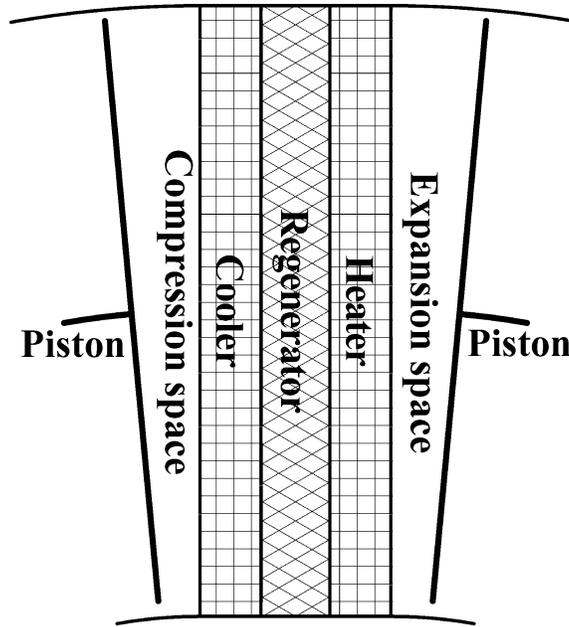
Figure 2. Schematic configuration of an Alpha type Stirling engine.

feature of the machine is that the power piston is actually realized with a flexible diaphragm, rather than with a sliding piston. This feature effectively eliminates leakage around the piston, and most significantly eliminates any need for lubrication, which is again consistent with the need for long-term maintenance free operation.

To the best of our knowledge, all existing free-piston designs are single-acting machines that have an inherent complexity and loss mechanism in the need to drive a displacer piston. Also, all existing double-acting multiple-piston machines incorporate pistons that are mechanically linked with a swashplate or other such mechanical linkage. As such, these machines are capable of delivering relatively high power density, but do not necessarily result in the low-cost low-loss system that we aim to realize.

The use of a multiple-phase, double-acting, free-piston machine has not been reported in the literature. A likely reason for this is the potential difficulty in coordinating the phasing among the pistons. Therefore, we discuss the design and analysis strategies of a multiple-phase Stirling engine system in this section.

3.1. Three-Phase Stirling Engine System Design

Stirling engines are categorized as Alpha, Beta and Gamma type engines.[7]   The two latter configurations incorporate a displacer between expansion and compression spaces. Furthermore, in these two configurations, working fluid has to flow through curved passages joining appropriate working spaces. Hence, in order to minimize the fluid flow losses along these curved passages and to eliminate the thermal leakage and mechanical friction losses associated with the displacer, the Alpha configuration, where heat exchangers (heater, cooler and regenerator) are aligned cylinders with the same radii, is considered for the present Stirling engine design, Fig. 2. In this configuration, the pistons have a skewed-phase sinusoidal motion where the efficiency and output power of the engine is a function of the phase delay between compression and expansion spaces.

Since we intend to extend the design to a multiple-phase configuration, we need to select a number of phases that are linked together to form the system. In other words, we need to specify the best phase delay between expansion and compression spaces. Thus, we select the case (among feasible phase delays) that has the highest efficiency. We considered identical operating conditions and performed second-degree (Adiabatic[7]) analysis on a prototype design for phase delay candidates of 60, 90 and 120 degrees which, respectively, are associated with six, four and three phase systems. The results of the mentioned simulations have been compared in Fig. 3 and readily suggest the three-phase engine system as the preferred design.
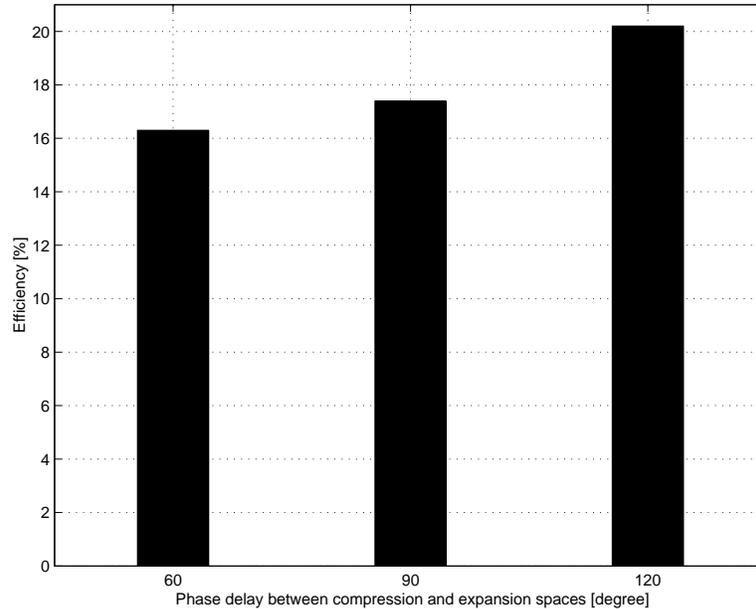
Figure 3. Calculated efficiency versus phase delay between compression and expansion spaces of a single engine for three, four, and six phase Stirling engine systems.

Engine dimensions were chosen based on very simple Beale analysis.[7] We initially intend to use ambient pressure air, which obviates the need for difficult working fluid retaining seals. Operation in the range of 50 Hz is also considered due to the feasibility of achieving a gas-spring-mass resonance in this range, the documented successful Stirling machine work in this frequency range, and the convenience of implementing a simple voice-coil type generator that operates at this frequency. In fact, fluid flow correlation data suggests lower frequencies can lead to higher thermodynamic efficiencies, but at the expense of reduced power output and a more costly generator element.

Dynamic behavior of the three-phase configuration also must be studied to ensure the potential of having expected operating characteristics: symmetrical three-phase steady state operation and self-starting capability. To do so, the first-degree (Isothermal[7]) model of a Stirling engine was reformulated for a three-phase design. Fig. 4(a) shows an eigenvalue plot in the complex plane, with eigenvalues numerically calculated for the linearized three-phase system. The complex pair in the right half plane corresponds to forward three-phase operation in generation mode. Since this mode is unstable, it will spontaneously grow until a loading mechanism (the generator and rectifier system) absorbs mechanical power at the same rate that mechanical power is produced. This is the intended mode of operation. Also of interest is the complex pair of eigenvalues in the left half plane. This pair corresponds to backward three-phase operation where mechanical power needs to be supplied at this resonant frequency to support the motion. This mode corresponds to operation as a Stirling heat pump. The third pair of eigenvalues located directly on the complex axis, correspond to a "zero-sequence" or simple oscillation mode where none of the working gas volumes undergoes any expansion or compression. Rather, each of the gas volumes is simply shuttled back and forth (in phase) through its respective regenerator. Although this latter mode is of no interest from a thermodynamic point of view, it is useful in allowing an independent assessment of fluid flow losses. Fig. 4(b) shows how each piston assembly develops its motion at start-up, whereas Fig. 4(c) displays the motions of the three independent piston assemblies on the same graph during the start-up transient. Convergence to a balanced three-phase steady state operation is illustrated in Fig. 4(d).

3.2. Losses in Stirling Engine

There are a number of loss contributors in a Stirling engine system, including ineffectiveness in the heat exchangers (i.e. the heater, cooler, and regenerator), fluid flow losses in these elements, mechanical friction losses, and
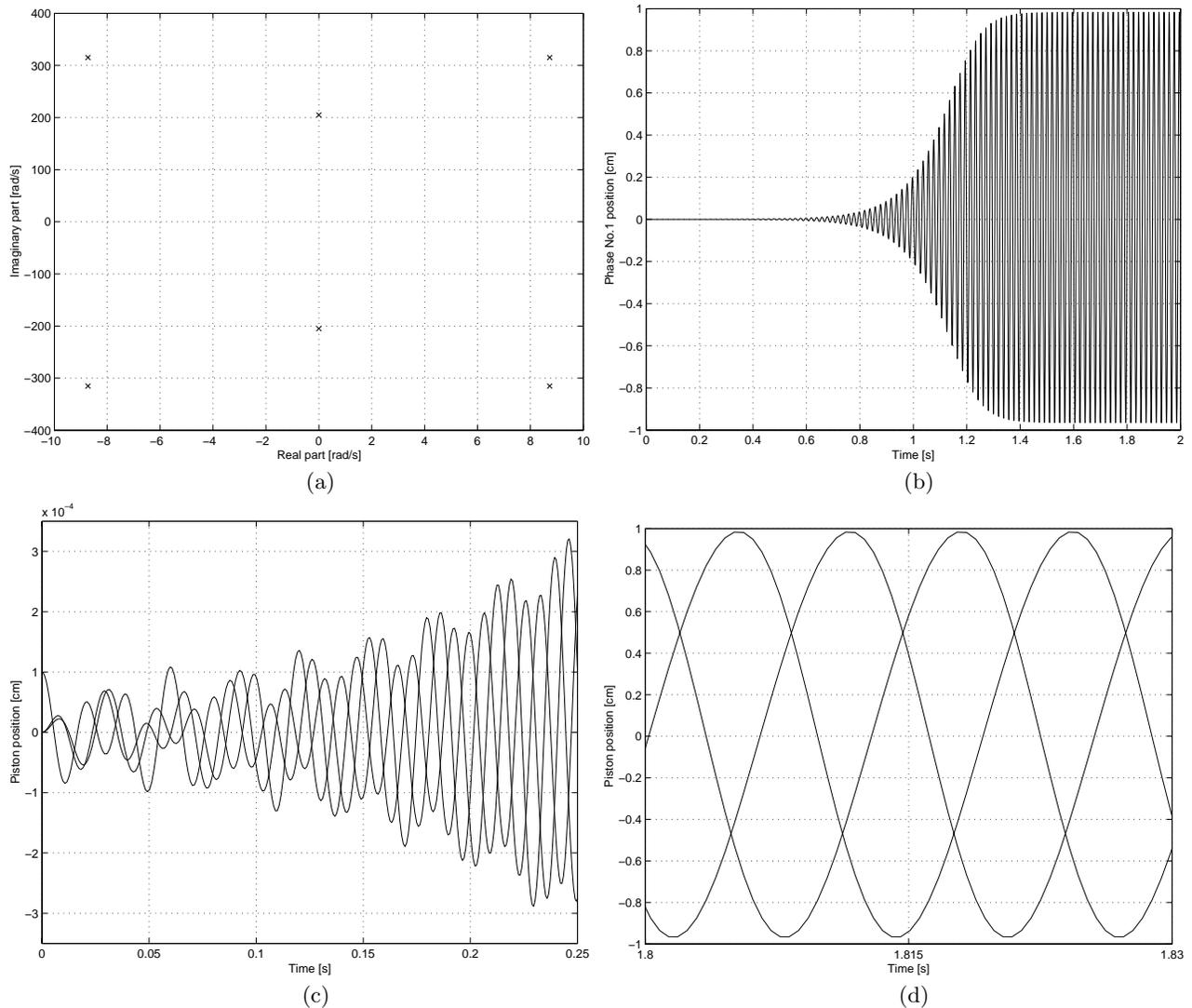
Figure 4. Dynamic simulation of three-phase system. **(a)** Eigenvalue analysis result of the three-phase Stirling engine system. **(b)** Phase No. 1 position. **(c)** System develops its motion starting from a slight perturbation, indicating potential for self-start. **(d)** After startup in (c), system reaches its three-phase steady state operating condition.

static heat loss. Heater and cooler ineffectiveness can be thought of as temperature drops associated with the heater and cooler, respectively, that directly affect system efficiency by degrading the available Carnot efficiency. Regenerator ineffectiveness can be analyzed as a thermal heat loss since it manifests itself in placing extra thermal load on the heater and cooler. On the other hand, fluid flow losses are supplied as a fraction of the available mechanical output power.

Mechanical friction is virtually eliminated by replacing moving pistons by diaphragms. Thus, losses associated with surface-to-surface friction and lifetime limitations associated with mechanical wear are avoided. As a further consequence, it will enable the engine system to self-start upon application of heat.[11] Sudden expansion and contraction is another source of loss that results from unequal heater, cooler, or regenerator diameters.[12] In order to prevent this type of loss, equal-diameter heat exchangers are considered in this design.

Due to the temperature differential from heater to cooler, some heat is lost from the heater by thermal leakage through the regenerator. By increasing the thermal resistance of the regenerator housing, one can minimize this
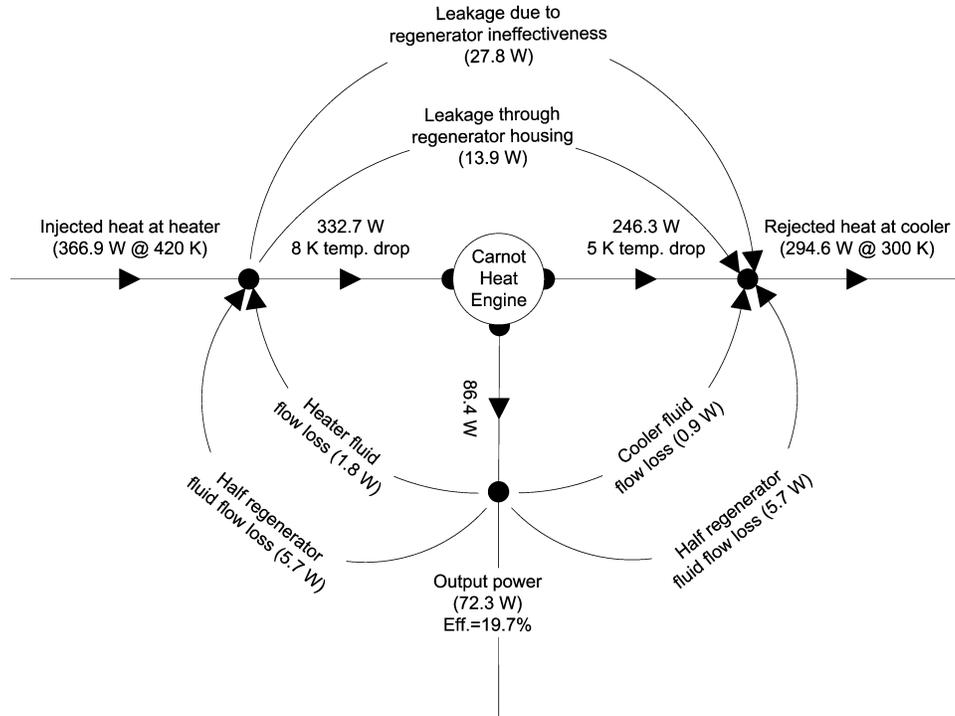
Figure 5. Power balance diagram of the designed Stirling engine.

loss. This can be achieved by choosing a good thermal insulating material for the regenerator housing and by decreasing the housing cross-section to a minimal mechanical dimension. We note that low cost organic materials are appropriate for this low temperature application.

A good heat exchanger should provide enough surface area to transfer the required heat to the working fluid with the least possible temperature drop and, at the same time, introduce the least possible flow friction (or pressure drop) loss. Since these are two competing requirements, a good design of heat exchanger maintains a reasonable balance between temperature and pressure drops. Based on our design criteria, wire screens appear to be the best option for the heat exchangers of the Stirling engine. In this section, we characterize the flow friction and convective heat transfer of such heat exchangers. It is worth noting that the regenerator is a column of woven wire screens with circular cross section, whereas the heater and cooler are columns of stacked wire screens (not woven) with square cross section.

Unfortunately, there is no strong theory behind the flow friction and heat transfer characteristics of wire screen exchangers. Rather, all available data are empirical correlations obtained from experiments on various fluids at various operating conditions. Some of these correlations have been compared in Ref. 13 and updated in Ref. 14. All compared correlations are for steady flow conditions, except the one by Tanaka.[15]   In addition to the summary and comparison, output power and efficiency analysis of the GPU-3 Stirling engine has been calculated[13] and compared with the experimental data.[7]   The analysis on the GPU-3 engine that is based on the Tanaka correlation is conservative with respect to actual experimental data.[13]   That is, the predicted efficiency based on the Tanaka correlation is actually exceeded by the experimental measurement. Furthermore, since the working fluid conditions reported on by Tanaka (e.g. temperature, pressure, fluid type, Reynolds number) fit in the range of conditions for the Stirling engine design discussed here, we have relied on the Tanaka correlations in our design computations.

A spreadsheet calculator has been assembled to help quickly adjust the design parameters of the Stirling engine. Based on a Schmidt analysis,[7]   it calculates the injected and rejected heats as well as output mechanical power of an Alpha Stirling engine with specified dimensions, working fluid and phase difference between expansion

and compression spaces. It also computes all the above mentioned power losses and temperature drops and adjusts the final results accordingly. Based on the spreadsheet analysis, we expect the three-phase Stirling engine system to produce about 217 W at 19.7% efficiency (that is about 70% of corresponding 28.6% Carnot efficiency). These are the efficiency data referred to previously. Figure 5 shows the power balance diagram of a single Stirling engine in the designed three-phase system. Further, the spreadsheet calculator predicts that output power and efficiency can be increased to 257 W and 19.3% (67% of corresponding Carnot efficiency) by using helium as working fluid. Or, power output can be increased to 2.75 kW at an efficiency of 18.7% by increasing the working fluid (air) pressure to 10 bars.

CONCLUSION

We have outlined a promising case for the use of distributed solar-thermal-electric generation, based on low temperature differential Stirling engine technology in conjunction with state-of-the-art solar thermal collectors. Although the predicted efficiencies are modest, the estimated cost in $/W for large scale manufacturing of these systems is quite attractive in relation to conventional photovoltaic technology. In an on-going program at UC Berkeley, experimentation with representative prototype systems is in progress.

ACKNOWLEDGMENTS

REFERENCES

1. W. T. Welford and R. Winston, *High Collection Nonimaging Optics*, Academic Press, San Diego, 1989.
2. *Solar Electric Products Catalog: Solar Electric Modules, 10th Edition*, Kyocera Solar, Japan, 2003.
3. H. Schweiger, *The Potential of Solar Heat for Industrial Processes (POSHIP), Final Report, Project No. NNE5-1999-0308*, European Commission - Directorate General for Energy and Transport, European Union, 2001.
4. W. Callister, *Materials Science and Engineering: An Introduction*, Wiley, New York, 2003.
5. *G Series Solar Collectors Technical Specifications*, Thermo Dynamics, Canada, 1999.
6. *SOLEL-CPC 2000, Colector Solar Termico de Concentracion*, Siemens Controlmatic, Barcelona, 2000.
7. I. Urieli and D. M. Berchowitz, *Stirling Cycle Engine Analysis*, Adam Hilger, Bristol, 1984.
8. G. T. Reader and C. Hooper, *Stirling Engines*, E. and F.N. Spon, London; New York, 1983.
9. Walker and J. R. Senft, *Free Piston Stirling Engines*, Springer-Verlag, Berlin; New York, 1985.
10. T. Finkelstein and A. J. Organ, *Air Engines: The History, Science, and Reality of the Perfect Engine*, ASME Press, New York, 2001.
11. R. M. Erbeznik and M. A. White, "Test results and commercialization plans for long life stirling generators," *Proceedings of the 31st Intersociety Energy Conversion Engineering Conference* **2**, pp. 1265–1270, 1996.
12. I. Yamashita and K. Hamaguchi, "Effects of enterance and exit areas on the pressure drop and velocity distribution in regenerator matrix," *JSME International Journal* **series II, vol. 42, no. 3**, pp. 498–505, 1999.
13. B. Thomas, "Evaluation of 6 different correlations for the flow friction factor of stirling engine regenerators," *Proceedings of the 34th Intesociety Energy Conversion Engineering Conference* **no. 01-2456**, 1999.
14. B. Thomas and D. Pittman, "Update on the evaluation of different correlations for the flow friction factor and heat transfer of stirling engine regenerators," *Proceedings of the 35th Intesociety Energy Conversion Engineering Conference* **1**, pp. 76–84, 2000.
15. M. Tanaka, I. Yamashita, and F. Chisaka, "Flow and heat transfer characteristics of the stirling engine regenerator in an oscillating flow," *JSME International Journal* **series II, vol. 33, no. 2**, pp. 283–289, 1990.